https://doi.org/10.1016/j.image.2019.115644

Early Termination for Fast Intra Mode Decision in Depth Map Coding using DIS-inheritance

Chang-Hong Fu, *Member, IEEE,* Hao Chen, Yui-Lam Chan*, *Member, IEEE,* Sik-Ho Tsang, *Member, IEEE,* and Xiaohua Zhu, *Member, IEEE*

***Abstract*—Depth Intra Skip (DIS) mode is a new depth intra coding tool in the 3D extension of High Efficiency Video Coding (3D-HEVC) to improve the coding efficiency of depth maps. The optimization of quadtree partitioning in HEVC is conducted on different Coding Unit (CU) sizes from 64×64 to 8×8. Although all CU sizes should be considered in partition decision, only the CUs in the optimal partition structure are coded in the final bitstream. In this paper, it is found that the CUs well predicted by DIS (i) occupy a large proportion in mode decision; (ii) have a strong consistency in its sub-CUs at the higher depth level; and (iii) tend to be coded at the lower depth level in the final bitstream. Based on these observations, this work proposes an early termination scheme for fast intra mode decision in depth maps. Early termination of CU splitting is triggered according to the consistency of DIS between different depth levels by evaluating several most probable modes in the current CUs and its four sub-CUs based on the new distortion metric. Simulation results demonstrate that the proposed algorithm could save 31.04% of depth coding time with 0.07% increase in BDBR. By integrating with other fast intra mode decision methods, the overall algorithm could provide averagely 50.08% time reduction with only 0.64% increase in BDBR.**

***Index Terms*—3D-HEVC, depth map, depth intra skip mode, coding unit partitioning, view synthesis optimization**

I. Introduction

Depth intra coding in the 3D extension of High Efficiency Video Coding (3D-HEVC) [1] basically adopts the quadtree-based Coding Tree Unit (CTU) structure in HEVC [2]. The CTU is a basic unit and is divided into several Coded Units (CUs) that can be represented by a recursive quadtree structure. An optimal CU partition within a CTU is a combination of different square sizes ranging from 64×64 to 8×8 pixels [3]. In addition to the conventional 35 HEVC intra modes (CHIM) [4], several new depth intra coding tools such as Depth Intra Skip (DIS) mode [5], Depth Modelling Mode (DMM) [6], Segment-wise DC Coding (SDC) [7] and View Synthesis Optimization (VSO) [8] have been designed to code depth maps in 3D-HEVC. These new techniques improve the coding efficiency at the expense of dramatically increased computational complexity since it is necessary to find the best CU partitions for all possible CU combinations.

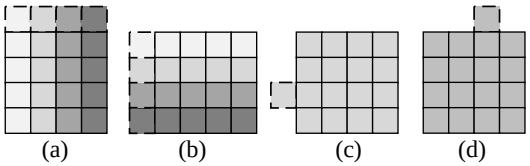

Fig. 1. An example of predicted CUs (solid line) with neighboring pixels (dotted line) by DIS. (a) DIS type 0, (b) DIS type 1, (c) DIS type 2, and (d) DIS type 3

To reduce the computational complexity of depth intra coding, many fast approaches have been proposed in the literature. They can be roughly divided into two categories: fast mode decision methods [9-26] and fast CU partitioning methods [27-29]. In [9-12], the complex DMM mode is skipped for smooth regions identified by block variances or the rough mode cost before DMM. The investigations in [13-14] proposed some methods to detect the simple edge regions where one of the traditional angular modes is efficient and the redundant DMM can then be skipped. The algorithms in [15-20] reduce the number of wedgelet patterns for DMM to be searched, where the block gradient, the variance, and the current best traditional angular mode are used to create the subsets for searching. In [21-22], the VSO metric is simplified. The algorithm in [21] estimated the VSO cost using an adaptive model for different pixel intervals. An area-based scheme for VSO calculation in [22] only requires co-located texture information. In [23-24], the number of candidates and search range for SDC are limited based on the mode information from the traditional residual quadtree. In [25], the number of mode candidates for both of the traditional residual quadtree and SDC checking in intra mode decision is limited based on statistical analysis. In our previous work [26], the VSO metric in DMM search is simplified as the Squared Euclidean Distance of Variances (SEDV), and a Probability-Based Early Decision (PBED) method was proposed to reduce the number of

This work was supported in part by Fundamental Research Funds for the Central Universities (No. 30917011319), and a grant from the Research Grants Council of the Hong Kong Special Administrative Region, China (Grant No. PolyU 152052/15E).

C. H. Fu, H. Chen, and X. Zhu are with the School of Electronic and Optical Engineering, Nanjing University of Science and Technology, Nanjing, 210019, CHINA (e-mail: enchfu@njust.edu.cn; 2323011088@qq.com; zxh@mail.njust.edu.cn).

Y. L. Chan, and S. H. Tsang are with the Centre for Signal Processing, Department of Electronic and Information Engineering, The Hong Kong Polytechnic University, Hong Kong, China (e-mail: enylchan@polyu.edu.hk; sik-ho.tsang@polyu.edu.hk).

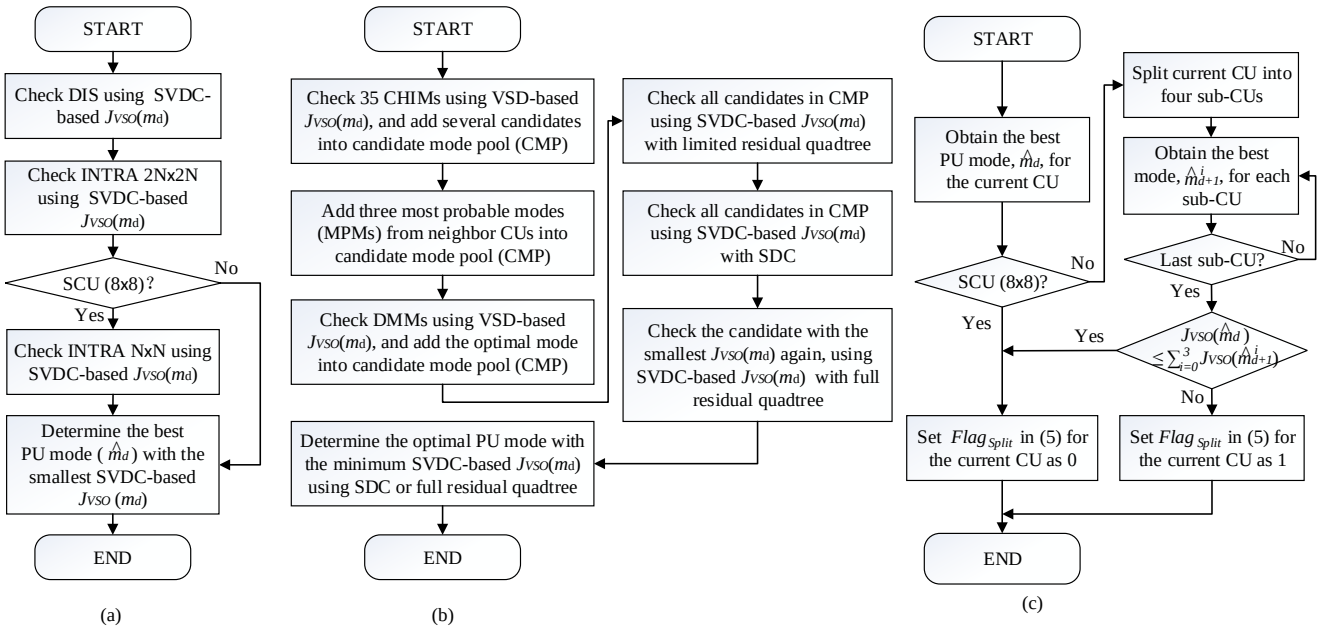

Fig. 2. Depth intra mode decision and partition decision: (a) PU mode decision for each CU; (b) mode decision for each PU of INTRA 2N×2N or INTRA N× N; and (c) CU partition decision for each CU.

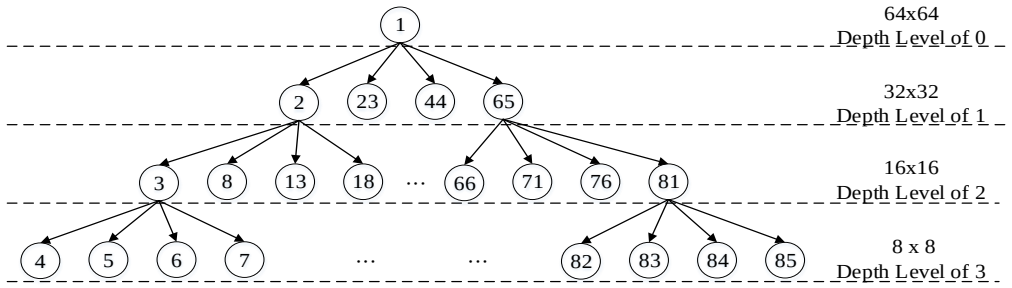

Fig. 3. An example of coding CU partitioning among different depth levels (the number in the circle is the compressing order of the CUs)

candidates in the final mode decision.

On the other hand, there are few fast algorithms designed for CU partitioning in depth map coding. Our previous work [27] limits the range of depth level based on corner point detection. An CU quadtree pruning algorithm was designed in [28] by considering the variance of CUs and the estimated distortion of the single depth intra mode. In [29], an inter-component coding tool was developed, where the depth coding quadtree is limited to the coded texture quadtree.

However, DIS, which is the most commonly used in intra mode, is seldom addressed in the current design of the fast methods, especially in the fast intra CU partitioning methods. Besides, the VSO process only aims at obtaining the best mode by evaluating the synthesized view distortion and its associated coding bits at certain depth level, and the relationship between different depth levels is never considered and utilized in the existing approaches. In this paper, by analyzing the distribution of DIS modes at each depth level, we will reveal that the CUs well predicted by DIS have a strong consistency in all its sub-CUs, in which the VSO computations are unnecessary. An early termination method for CU partitioning based on this consistency is then proposed to speed up the whole depth intra coding process. To the best of our knowledge, this is the first method that uses the prediction consistency between depth levels in DIS among the current fast CU partitioning methods for depth map coding.

The rest of this paper is organized as follows. In Section II, the background of DIS, depth intra mode decision and CU partitioning in 3D-HEVC are reviewed. In Section III, DIS distribution among various depth levels is analyzed, and the DIS-inheritance is then presented. Based on DIS-inheritance, the proposed fast method is proposed in Section IV. The experimental results and conclusion are given in Section V and Section VI, respectively.

II. Background And Motivation

In this section, the DIS mode, depth intra mode decision and CU partitioning process in 3D-HEVC are reviewed.

A. Depth Intra Skip Mode

DIS mode is a new intra mode for depth map coding [5], which is useful in coding flat regions. As illustrated in Fig. 1, DIS directly uses the reconstructed value of spatial neighboring CUs to represent the current CU. In DIS, no prediction residual is encoded, which is the major difference between DIS and other intra modes.

There are two vertical and two horizontal types of DIS, which is signaled by an index (DIS type 0-3). As shown in Fig. 1(a) and (b), the CUs predicted by type 0 and type 1 of DIS are the same as the vertical and horizontal angular modes in CHIMs,

respectively. On the other hand, type 2 and type 3 of DIS, as described in Fig. 1(c) and (d), construct a predicted CU with one single depth value from mid-left or mid-above pixel, respectively. Finally, the DIS prediction type with the minimum VSO cost is determined as the best DIS type for the current CU.

B. Depth Intra Mode Decision

For each CU, the Prediction Unit (PU) is further defined. The same prediction mode including DIS, CHIM and DMM is used inside each PU. At all CU depth levels (0~3), PU size is defined as the same as that of CU, which is called 2N×2N. Besides, when depth level equals to 3, i.e. the Smallest Coded Unit (SCU) of 8×8 pixels, additional PU type N×N is defined by further splitting SCU into four equally non-overlapped square units.

Instead of the traditional Rate Distortion Optimization (RDO), VSO is conducted in the PU mode decision for depth maps to guarantee the synthesized view quality [30], as follows:

$$J_{VSO}(m_d) = D_{VSO}(m_d) + \lambda \times R(m_d) \tag{1}$$

where m_d is one of the possible candidate modes at the depth level of d, the VSO cost $J_{VSO}(m_d)$ is computed by the distortion $D_{VSO}(m_d)$ plus the Langrangian multiplier λ times the coding rate $R(m_d)$. In VSO, $D_{VSO}(m_d)$ takes both the distortion of the synthesized view, $D_{syn}(m_d)$, and the distortion of the depth map, $D_{dep}(m_d)$, into consideration which is formulated as

$$D_{VSO}(m_d) = \frac{w_{syn} \times D_{syn}(m_d) + w_{dep} \times D_{dep}(m_d)}{w_{syn} + w_{dep}} \tag{2}$$

where w_{syn} and w_{dep} are the weighting factors of $D_{syn}(m_d)$ and $D_{dep}(m_d)$, respectively. $D_{dep}(m_d)$ is calculated by the sum of squared error (SSE) or sum of absolute Hadamard transform difference (SATD). The way to compute $D_{syn}(m_d)$ can either be computed by the rendering approach or the non-rendering approach. The Synthesized View Distortion Change (SVDC)-based VSO defined in [31] is considered as the rendering approach, which directly performs view synthesis using the encoded data and then measure the distortion of the synthesized view, $D_{syn}(m_d)$. This rendering approach requires higher computational complexity. The non-rendering approach, on the other hand, is the model-based view synthesis distortion (VSD) [32], which weights the depth distortion with the sum of absolute horizontal gradients of the co-located texture as follows:

$$D_{syn}(m_d) = \sum_{(x,y)\in PU} \left(\frac{1}{2} \cdot \alpha \cdot \left| s_{D(x,y)} - \tilde{s}_{D(x,y)}(m_d) \right| \cdot \left[\left| \tilde{s}_{T(x,y)} - \tilde{s}_{T(x-1,y)} \right| + \left| \tilde{s}_{T(x,y)} - \tilde{s}_{T(x+1,y)} \right| \right]^2 \right) \tag{3}$$

where (x, y) means the sample position in a PU. $s_{D(x,y)}$, and $\tilde{s}_{D(x,y)}(m_d)$ indicate the original and reconstructed depth maps, respectively. $\tilde{s}_{T(x,y)}$ indicates the reconstructed texture. (x, y) means the sample position in a PU. α is the proportional coefficient determined by the depth distance from the camera.

The PU intra mode decision is then simplified as the flowchart in Fig. 2(a). The INTRA 2N×2N or INTRA N×N mode includes CHIMs and DMMs, where the coding process is detailly described in Fig. 2(b). Firstly, a candidate mode pool (CMP) is constructed by checking CHIMs and DMMs, where the non-rendering or VSD-based $J_{VSO}(m_d)$ in (3) is used. Secondly, the candidates in CMP are checked using $J_{VSO}(m_d)$ with residual quadtree or SDC that employs the rendering or SVDC-based approach. Finally, the mode with the smallest $J_{VSO}(m_d)$ is determined as the best PU mode, $\hat{m}_d$, as shown in (4).

$$\hat{m}_d = argmin_{m_d \in M_d}(J_{VSO}(m_d)) \tag{4}$$
$$M_d = \{DIS, CMP\} = \{DIS, CHIM, DMM\}$$

where M_d is the set of modes with DIS, CHIM and DMM.

C. CU Partitioning of Depth Intra Coding

In 3D-HEVC, depth maps are firstly divided into non-overlapping CTUs. Each CTU can be a maximum of 64×64 pixels. Starting from CTU, the quadtree CU partitioning allows the CTU recursively splitting into four equally sized CUs until the SCU is reached. As shown in Fig. 3, all possible CU sizes are tested during the CU partitioning process to obtain the best coding efficiency. However, not all CUs are coded in the final bitstream. The splitting of CU is determined by comparing the VSO cost of the larger CU, $CU(\hat{m}_d)$, at the depth level of d, $J_{VSO}(\hat{m}_d)$ and the sum of VSO costs of four smaller sub-CUs, i.e. $CU(\hat{m}^i_{d+1})$ for $i \in \{0,1,2,3\}$, at the higher depth level of d+1, $\sum_{i=0}^{3} J_{VSO}(\hat{m}^i_{d+1})$, according to

$$Flag_{Split} = \begin{cases} 0, & if \quad J_{VSO}(\hat{m}_d) \le \sum_{i=0}^{3} J_{VSO}(\hat{m}^i_{d+1}) \\ 1, & if \quad J_{VSO}(\hat{m}_d) > \sum_{i=0}^{3} J_{VSO}(\hat{m}^i_{d+1}) \end{cases} \tag{5}$$

where the $Flag_{Split}$ of 0 and 1 represent Non-Split and Split, respectively, for the current CU.

The flowchart in Fig. 2(c) describes the partition decision of each CU. Taking the CU 3 in Fig. 3 as an example, if the total VSO cost of its sub-CUs (CU 4-7) is larger than the VSO cost of CU 3, the CU 3 will not split into sub-CUs in the final structure as the decision in (5). Otherwise, the CU 4-7 will replace the CU 3 as the optimal partition modes of the current CU. The same decision is employed for all CUs recursively from high to low depth levels. Finally, the partition structure with the minimum VSO cost is selected as the optimal structure and coded in the bitstream.

It is noted that no matter what the final partition structure is, there are 85 times recursive computation for all possible CUs within one CTU in the worst case, as shown in Fig. 3. However, not all CUs are necessary to be checked. Early termination of the partitioning process could significantly reduce the computational complexity.

D. Complexity of Depth Intra Coding

Since tremendous candidates are considered in depth intra-mode decision and CU partitioning, the depth map coding

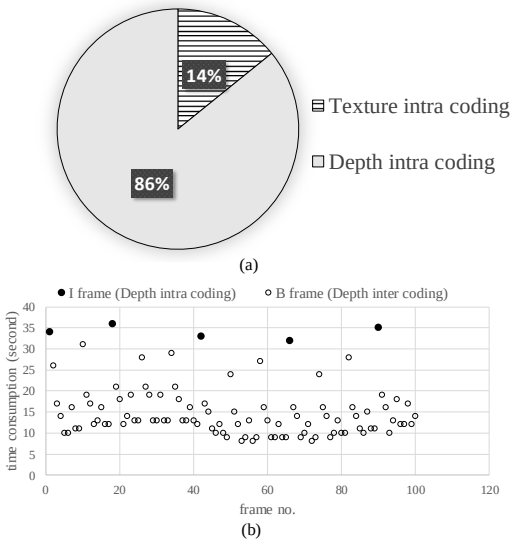

Fig. 4. Encoding time of depth intra coding compared with (a) texture intra coding in *All-intra* configuration and (b) depth inter coding in *Random-access* configuration.

occupies about 86% of total 3D-HEVC encoding time, as illustrated in Fig. 4(a), in which *All-intra* configuration in HTM-16.0 is used. As shown in the figure, the time consumption of depth intra coding is six times that of texture intra coding. At the same time, when *Random-access* configuration is employed, it is demonstrated in Fig.4(b) that the time consumption of intra frame is obviously higher than that of inter frames. From Fig. 4(a) and Fig. 4(b), we can conclude that the need for accelerating mode decision in depth intra coding is crucial in the context of 3D-HEVC.

The motivation of reducing complexity in depth intra coding could also be found in [9]-[26]. In these works, *All-intra* is the most commonly used configuration in Common Test Condition (CTC) [34] to evaluate the performance of fast intra prediction algorithms since the acceleration effect of fast intra algorithms could be demonstrated better as compared with other conditions such as *Random-access*. As a result, all existing algorithms in [9]-[26] only show the results using *All-intra* configuration.

III. Observations of DIS-Inheritance

In this section, the DIS distributions at various depth levels are shown in both of the mode decision and the final bitstream. It is found that more CUs with DIS as the best mode are not coded in the final bitstream as the depth level increases. The DIS-inheritance is then introduced to relate the early termination of the CU partition decision in 3D-HEVC. All statistical analyses in this section are employed under the condition that will be described in Section V in detail.

A. DIS Distributions at Various Depth Levels and Their Relationship to Optimal mode

As mentioned above, DIS is the most dominant mode in depth intra coding. Table I shows the percentage of CUs that select DIS as the best mode in the mode decision of each depth level, $P\big(CU(\hat{m}_d = DIS)\big)$. From this table, it can be found that $P\big(CU(\hat{m}_d = DIS)\big)$ increases from 62.82% to 97.50% as the depth level increases. Besides, the percentage of CUs, which are coded as DIS mode at each depth level in the final bitstream, $P\big(CU(m_d^* = DIS)\big)$, is also shown. It is noted that m_d^* is the optimal mode among all depth levels, while $\hat{m}_d$ is only the best mode at the depth level of d. $P\big(CU(m_d^* = DIS)\big)$ decreases sharply from 57.16% to 1.17% as the depth level increases. At the depth level of 3, it is seen that only 1.17% in average of CUs are coded as DIS in the final bitstream even though there is a very high percentage, 97.50% in average, of DIS mode is chosen in mode decision at that level. These statistics show that more CUs coded as DIS are unnecessary to be checked as the depth level increases. It could help the early termination of CU partitioning.

B. DIS-Inheritance

An example of DIS in mode decision at each depth level is depicted in Fig. 5. In this figure, the CUs where DIS is selected as the best mode at the current depth level, are marked as gray. As illustrated in this example, the CUs well predicted by DIS are more likely to select DIS at the next depth level. This kind of consistency, in this paper, is named as DIS-inheritance, as shown in the CUs surrounded by the dotted lines in Fig. 5. The DIS-inheritance could last from the current depth level to the highest one (SCU). The CUs inheriting from lower depth levels

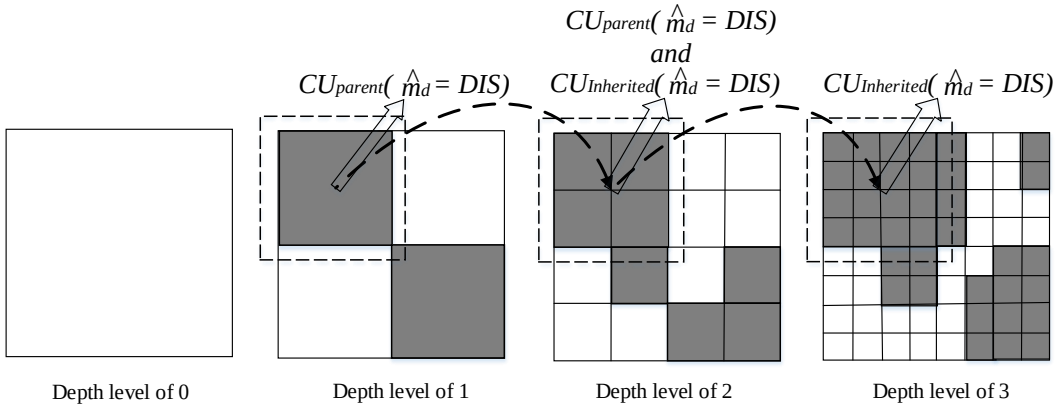

Fig. 5. An example of CUs coded by DIS (in gray) and DIS-inheritance (surrounded by dotted line) at each depth level

are defined as DIS-inherited CUs, $CU_{Inherited}(\hat{m}_d = DIS)$, while the corresponding CUs being inherited at lower levels are called DIS-parent CUs, $CU_{Parent}(\hat{m}_d = DIS)$, as the following conditions:

$$CU_d \in CU_{Parent}(\hat{m}_d = DIS), \quad if\ \ CU(\hat{m}_d = DIS)\ and\ CU\left(\hat{m}^i_{d+1} = DIS \middle| i = 0,1,2,3\right) \quad (6)$$

and

$$CU_d \in CU_{Inherited}(\hat{m}_d = DIS), \quad if\ \ CU_{d-1} \in CU_{Parent}(\hat{m}_d = DIS) \quad (7)$$

where CU_d is the CU at the depth level of d.

In fact, the DIS-inherited CUs are the CUs that directly use the reconstructed value of their spatial neighboring pixels as their DIS-parent CUs. As a result, these DIS-inherited CUs keep the similar distortion as their corresponding DIS-parent CU at the lower depth level. However, the rate term $R(m_d)$ increases when the depth level increases. It is due to the increasing number of CUs for the same region at the higher depth level. More bits are consumed in the syntax for more complicated partition structure. The total VSO costs of DIS-inherited CUs is obviously larger than the VSO cost of their corresponding DIS-parent CU at the lower level. Consequently, those CUs should be coded as DIS mode at the lower level and the early termination of CU partitioning can be carried out when DIS-parent CUs are detected.

To further observe the impact of DIS-inheritance on the CU partition decision, we analyze the percentage of DIS-parent CUs choosing to split into smaller CUs, $P(CU_{Parent}(\hat{m}_d = DIS) \mid Flag_{Split} = 1)$, as shown in Table II. $P(CU_{Parent}(\hat{m}_d = DIS) \mid Flag_{Split} = 1)$ keeps a very low percentage at various depth levels from 2.27% to 0.10%. This observation verifies that most DIS-parent CUs are not split in the final bitstream. Thus, for DIS-parent CUs, all the related recursive computation of mode decision for the corresponding smaller CUs are unnecessary. In addition, the percentage of DIS-parent CUs at various depth level, $P(CU_{Parent}(\hat{m}_d = DIS))$, are also shown in Table II. At each depth level, the DIS-inheritance is believed to exist when the condition of (6) is satisfied. As we can see, $P(CU_{Parent}(\hat{m}_d = DIS))$ at different depth levels occupies has a significant percentage, from 56.39% to 90.91%. It means that DIS-parent CUs occupy a large proportion of CUs at each depth level. According to the small percentage of $(CU_{Parent}(\hat{m}_d = DIS) \mid Flag_{Split} = 1)$, the large amount of DIS-parent CUs can stop the partitioning. Based on the analysis in Table II, an early termination of depth intra CU partitioning based on DIS-inheritance is then proposed by detecting the DIS-parent CU in the next section.

TABLE I. PERCENTAGE OF DIS-CUS CHOSEN IN MODE DECISION AND CODED IN THE FINAL BITSTREAM

Test Seq.	$P(CU(\hat{m}_d = DIS))$ (%)				$P(CU(m^*_d = DIS))$ (%)			
	d=0	*d*=1	*d*=2	*d*=3	*d*=0	*d*=1	*d*=2	*d*=3
Kendo	45.88	70.05	87.27	95.84	42.67	15.50	5.46	1.51
Hall2	79.15	91.78	97.34	99.28	75.59	8.29	1.99	0.43
Dancer	63.41	81.59	92.09	97.39	53.22	16.49	5.95	1.57
Average	62.82	81.14	92.23	97.50	57.16	13.43	4.47	1.17

TABLE II. PERCENTAGE (%) OF DIS –PARENT CUS CHOSEN IN MODE DECISION AND CHOOSING TO SPLIT IN THE FINAL BITSTREAM

Test Seq.	$P(CU_{Parent}(\hat{m}_d = DIS))$			$P\left(\begin{matrix}CU_{Parent}(\hat{m}_d = DIS) \\ \mid Flag_{Split} = 1\end{matrix}\right)$		
	d=0	*d*=1	*d*=2	*d*=0	*d*=1	*d*=2
Kendo	40.31	66.77	85.70	0.86	0.32	0.11
Hall2	75.13	90.23	96.87	1.66	0.36	0.06
Dancer	53.73	76.17	90.15	4.29	1.07	0.14
Average	56.39	77.72	90.91	2.27	0.58	0.10

TABLE III. PERCENTAGE OF SUB-CUS HAVING THE BEST MODE INHERITED FROM THE CANDIDATE MODE LIST OF THE CURRENT CU

Test Sequence	$P(\hat{m}^i_{d+1} \in M_d)$ (%)		
	d=0	*d*=1	*d*=2
Kendo	84.77	98.09	99.50
Poznan_Hall2	96.40	99.68	99.92
Undo_Dancer	90.16	98.84	99.71
Average	90.44	98.87	99.71

TABLE IV. PERCENTAGE OF CUS WHERE THE RATE TERM $R(m^i_{d+1})$ OF DIS IS SMALLER THAN THAT OF OTHER MODES IN MODE DECISION

Test Sequence	$P(R(m^i_{d+1} = DIS) \le R(m^i_{d+1} \neq DIS))$ (%)		
	d=0	*d*=1	*d*=2
Kendo	99.76	99.78	99.92
Poznan_Hall2	99.95	99.97	99.99
Undo_Dancer	99.89	99.92	99.97
Average	99.86	99.89	99.96

IV. PROPOSED ALGORITHM

In Section III, we find that the DIS-inheritance exists across different depth levels, and the DIS-parent CUs seldom split into smaller CUs. Therefore, it is highly desired to use the DIS-inheritance to design an early termination scheme of CU partitioning. In this Section, we first introduce a method to detect DIS-parent CUs without further quadtree partitioning. The early-termination algorithm is then proposed based on the detected DIS-parent CU.

A. Determination of DIS-parent CUs

The key issue of the proposed algorithm is to detect the DIS-parent CUs at the current depth level according to the definition described in (6). In other words, the current CU is considered as a DIS-parent CU when the current CU and its four sub-CUs are all coded as DIS. In this paper, we consider the DIS-inheritance by estimating the VSO costs of DIS on both of the current CU and its four sub-CUs.

Practically, the best mode of the current CU can be selected by the traditional process in 3D-HEVC using (4). When the VSO cost of DIS is the smallest among all candidate modes in M_d, DIS is selected as the best mode. On the contrary, as shown in Fig. 3, estimating the best modes of its sub-CUs involves further partitioning to smaller units and could not be conducted at the current depth level due to the recursive process of 3D-HEVC. Thus, without conducting the original mode decision of the sub-CUs at the next level, an approximated method to simulate the mode decision of those four sub-CUs at the next level using the information from the CU at the current depth level is proposed in this paper, which is named as Approximate View Synthesis Optimization (AVSO).

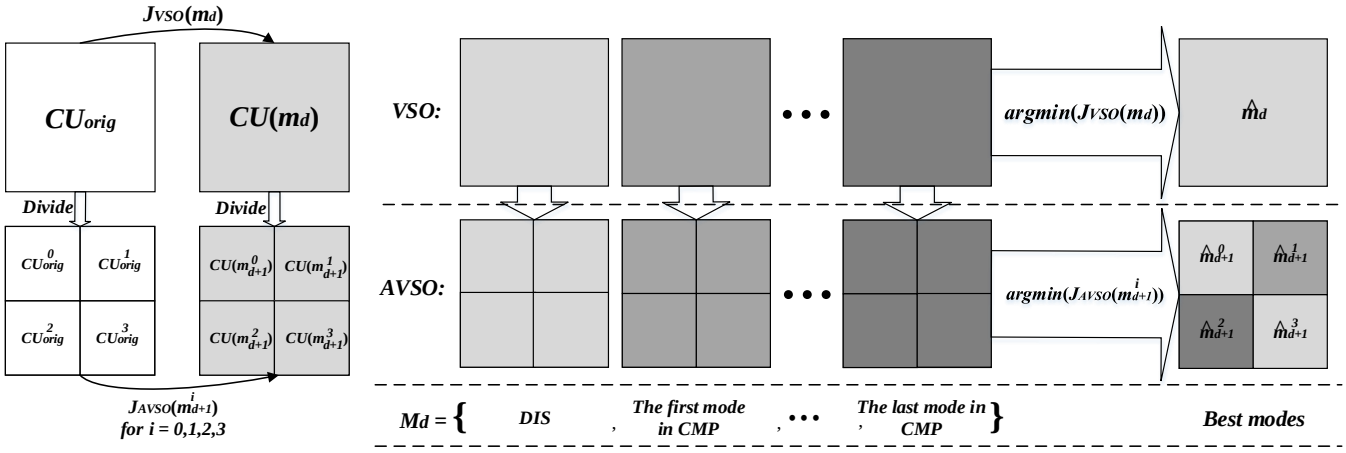

(a) (b)

Fig.6 An illustration (a) using AVSO to estimate VSO costs of sub-CUs, and (b) to obtain the five best modes of the current CU, and its four sub-CUs.

B. Approximate View Synthesis Optimization for Sub-CUs

As we can see the traditional optimization of mode selection in 3D-HEVC shown in Fig. 2(b), the best mode $\hat{m}_d$ of the current CU is selected from the modes listed in M_d of (4). The mode with the minimum SVDC-based VSO cost is decided as the best mode. In contrast, the set of modes at the depth level of d+1 for each sub-CU, M_{d+1}, could not be constructed at the time when the CU is encoded at the depth level of d. However, in this paper, we reveal the depth-level correlation between the current CU and its sub-CUs is very high in which the best mode of each sub-CU, $\hat{m}^i_{d+1}$, at the higher depth level of $d+1$ mostly exists in M_d of the CU at the current depth level of d. Table III then analyzes the percentage of sub-CUs whose $\hat{m}^i_{d+1}$ is one of the candidates in M_d of the current CU, $P(\hat{m}^i_{d+1} \in M_d)$. In this table, most of the sub-CUs, from 90.44% to 99.71%, can obtain their $\hat{m}^i_{d+1}$ from M_d of the current CU. In other words, the mode decision for sub-CUs could be estimated as selecting the best mode from M_d by calculating the VSO cost of each sub-CU. In other words, M_{d+1} can be approximated by M_d, as follows:

$$m^i_{d+1} \in M_{d+1} \sim M_d \quad (8)$$

For the detection of the DIS-parent CU, the requirement is to evaluate whether DIS is the best mode of all its sub-CUs by checking

$$J_{VSO}(m^i_{d+1} = DIS) < J_{VSO}(m^i_{d+1} \neq DIS) \text{ for } i = 0,1,2,3 \quad (9)$$

By putting (1) into the inequality (9), which can then be rewritten as

$$D_{VSO}(m^i_{d+1} = DIS) + \lambda \times R(m^i_{d+1} = DIS) < D_{VSO}(m^i_{d+1} \neq DIS) + \lambda \times R(m^i_{d+1} \neq DIS) \quad (10)$$

In (10), the rate terms, $R(m^i_{d+1} = DIS)$ and $R(m^i_{d+1} \neq DIS)$, however, cannot be obtained at the depth level of d. It is noted that DIS does not encode the prediction residual and it takes the fewest bits to encode. Table IV analyzes the percentage of CUs where $R(m^i_{d+1} = DIS)$ is the smallest among all intra modes in the mode decision at each depth level. It is observed that $R(m^i_{d+1} = DIS)$ is always smaller than that of other modes, i.e. $P(R(m^i_{d+1} = DIS) \leq R(m^i_{d+1} \neq DIS))$ is very large, more than 99.8% for all depth levels. Based on the analysis in Table IV, it is a high chance that $R(m^i_{d+1} = DIS)$ and $R(m^i_{d+1} \neq DIS)$ can be formulated as

$$R(m^i_{d+1} \neq DIS) - R(m^i_{d+1} = DIS) = \Delta R \geq 0 \quad (11)$$

By substituting (11) into (10), the checking condition becomes

$$D_{VSO}(m^i_{d+1} = DIS) < D_{VSO}(m^i_{d+1} \neq DIS) + \lambda \times \Delta R \quad (12)$$

which implies that if we can find the following condition (13),

$$D_{VSO}(m^i_{d+1} = DIS) < D_{VSO}(m^i_{d+1} \neq DIS) \quad (13)$$

The condition of (12) could be satisfied as ΔR is over 99.80% greater than zero as tabulated in Table IV. From (13), we can conclude that whether DIS is the best mode for the sub-CUs, $\hat{m}^i_{d+1}$, can be decided by considering the distortion term, $D_{VSO}(m^i_{d+1})$, only. Thus, we define an approximate VSO cost $J_{AVSO}(m^i_{d+1})$ with only the distortion term as (14) shows. And the best mode for each sub-CU is then decided by minimizing $J_{AVSO}(m^i_{d+1})$ as shown in (15).

$$J_{AVSO}(m^i_{d+1}) = D_{VSO}(m_{d+1}) \quad (14)$$

$$\hat{m}^i_{d+1} = argmin_{m^i_{d+1} \in M_{d+1}} J_{AVSO}(m^i_{d+1}) \quad (15)$$

According to (8), M_{d+1} can be approximated by M_d in the mode decision of (15). The termination condition of (15) can be further replaced by

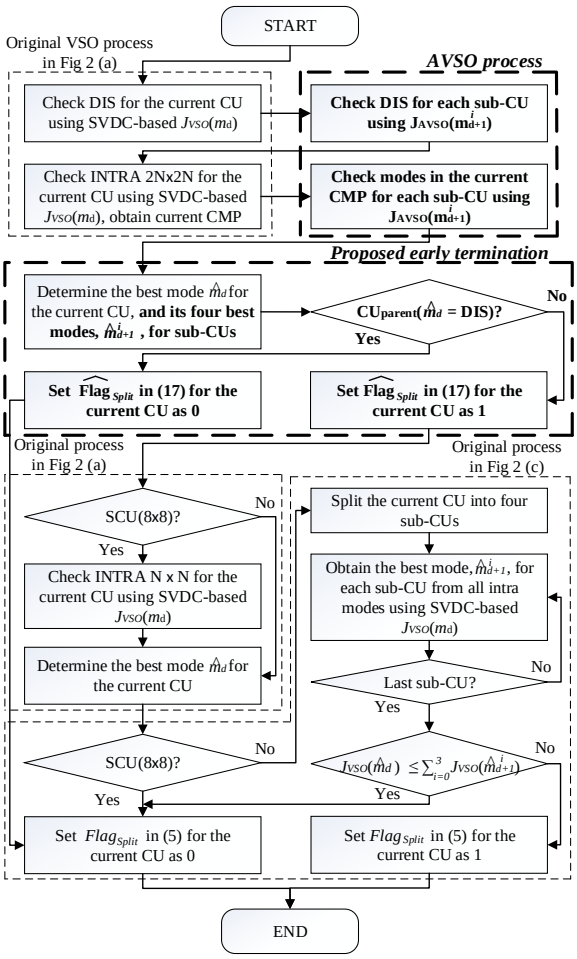

Fig.7 Flowchart of the proposed algorithm

$$\hat{m}_{d+1}^{i} = argmin_{m_{d+1}^{i} \in M_d} J_{AVSO}(m_{d+1}^{i}) \qquad (16)$$

The AVSO method calculated at the current depth level for the sub-CUs illustrated in Fig. 6(a). For each candidate mode m_d in M_d, there is a corresponding predicted CU, $CU(m_d)$, which is used to calculate the distortion from the original block, CU_{orig}, by minimizing SVDC-based $J_{VSO}(m_d)$ in (4). At the current depth level, the four corresponding predicted sub-CUs of m_{d+1}^{i} can be estimated by dividing the current predicted CU into four parts, $CU(m_{d+1}^{i})$ for $i = 0,1,2,3$. The distortion for each sub-CU is then calculated separately from the original sub-block, CU_{orig}^{i} for $i = 0,1,2,3$ using the AVSO process proposed in (16). To restrict the computational complexity of the AVSO process, the calculation of $D_{VSO}(m_{d+1}^{i})$ in (14) adopts the VSD-based distortion in (3). The four values are then used to estimate the real VSO cost for sub-CUs in the recursive coding process at the next depth level. Among all modes in M_d, each sub-CU will select the mode with the smallest $J_{AVSO}(m_{d+1}^{i})$ as its best mode, as defined in (16). By using AVSO, the best modes of the four sub-CUs at the depth level of $d+1$ can be obtained at the depth level of d.

TABLE V. CONFUSION MATRIX OF BINARY CLASSIFICATION

CUs decided to be	Not split by (17)	Split by (17)
Not split by (5)	TP	FN
Split by (5)	FP	TN

C. Proposed Early Termination of Block Partitioning

With the above formulations, the proposed algorithm based on DIS-inheritance is proposed as follows. In the conventional mode decision of each CU, several intra modes are selected into M_d. The mode with the smallest SVDC-based VSO cost from the M_d is then selected as the best mode of the current CU. From (8), the modes in M_d are also assumed to be M_{d+1} for the corresponding four sub-CUs in the proposed algorithm, as in Fig. 6(b). Then, the AVSO cost $J_{AVSO}(m_{d+1}^{i})$ is calculated to determine the best mode of each sub-CU, $\hat{m}_{d+1}^{i}$, in the AVSO process. Finally, the five best modes are decided for the current CU and its four sub-CUs. If all of the five best modes are DIS, the current CU is considered as a DIS-parent CU, having DIS-inheritance inside all its corresponding sub-CUs. Particularly, for SCUs at the depth level of 3, the AVSO process is also conducted for four sub-PUs (4×4). If the best modes of the current 8×8 PU and its four 4×4 PUs are all DIS after VSO and AVSO processes, then the current SCU is defined as a DIS-parent CU. Further splitting in the traditional intra coding process is never considered once a DIS-parent CU is detected.

The overall flowchart is described in Fig. 7. The bold part is from the proposed scheme, while the others are original steps in 3D-HEVC. At each CU depth, the best modes of the current CU and its four sub-CUs are decided using VSO and AVSO respectively. If the condition of DIS-parent CU in (6) is fulfilled, the CU partitioning at the depth levels of 0-2 or PU partitioning at the depth level of 3 is immediately terminated as in the following:

$$\widehat{Flag}_{Split} = \begin{cases} 0, & if\ CU_d \in CU_{Parent}(\hat{m}_d = DIS) \\ 1, & Otherwise \end{cases} \qquad (17)$$

TABLE VI. PRECISION AND RECALL OF THE PROPOSED BINARY CLASSIFICATION OF PARTITION TERMINATION BASED ON DIS-INHERITANCE

Test sequence	64×64 (d=0)		32×32 (d=1)		16×16 (d=2)		8 ×8 (d=3)	
	Recall (%)	Precision (%)	Recall (%)	Precision (%)	Recall (%)	Precision (%)	Recall (%)	Precision (%)
Balloons	56.49	97.92	47.10	99.70	54.50	99.90	66.11	100.00
Kendo	56.65	97.70	52.32	99.70	61.73	99.89	73.20	100.00
Newspaper	40.09	93.66	31.49	98.77	40.67	99.69	54.15	99.98
GT_Fly	52.71	98.46	62.66	99.89	77.44	99.97	86.72	100.00
Poznan_Hall2	69.93	98.16	76.41	99.72	85.93	99.95	92.03	100.00
Poznan_Street	19.13	87.91	27.46	98.49	49.96	99.77	65.06	99.99
Shark	61.80	90.58	59.21	98.69	69.73	99.42	78.67	99.97
Undo_Dancer	36.83	89.27	51.75	98.38	66.62	99.81	79.45	99.99
Average	**49.20**	**94.21**	**51.05**	**99.17**	**63.32**	**99.80**	**74.42**	**99.99**

TABLE VII. PERFORMANCE OF [26], [29], THE PROPOSED AND RESTRICT PROPOSED ALGORITHMS COMPARED WITH HTM-16.1

Test sequence	SEDV in [26] (%)		PBED in [26] (%)		Mora's[29] (%)		PRO (%)		Restrict-PRO (%)	
	ΔBDBR	ΔT	ΔBDBR	ΔT	ΔBDBR	ΔT	ΔBDBR	ΔT	ΔBDBR	ΔT
Balloons	+0.10	-15.67	+0.45	-27.16	+10.72	-45.41	+0.03	-22.83	+0.06	-19.71
Kendo	+0.17	-14.88	+0.12	-31.35	+1.66	-53.61	+0.07	-29.42	+0.04	-25.55
Newspaper	+0.23	-16.00	+0.56	-24.99	+4.40	-45.03	+0.14	-17.77	+0.08	-15.45
GT_Fly	+0.09	-14.84	+0.17	-33.84	+0.20	-53.20	+0.21	-51.99	+0.01	-42.76
Poznan_Hall2	+0.22	-11.99	+0.78	-43.75	+4.02	-63.75	+0.74	-58.10	+0.25	-48.41
Poznan_Street	+0.10	-14.57	+0.15	-33.44	+1.70	-50.04	+0.07	-28.90	+0.02	-26.52
Shark	+0.05	-15.57	+0.34	-26.57	+1.30	-50.12	+0.29	-40.95	-0.02	-33.90
Undo_Dancer	+0.03	-14.41	+0.39	-33.55	+1.01	-46.20	+1.28	-40.82	+0.15	-36.04
Average	**+0.12**	**-14.74**	**+0.37**	**-31.83**	**+3.13**	**-50.92**	**+0.35**	**-36.35**	**+0.07**	**-31.04**

TABLE VIII. PERFORMANCE OF [26], RESTRICT PROPOSED ALGORITHMS INTEGRATED WITH METHODS IN [12] COMPARED WITH HTM-16.1

Test sequence	SEDV+ PBED(%)		SEDV+ Restrict-PRO (%)		PBED + Restrict-PRO (%)		SEDV+PBED+ Restrict-PRO (%)	
	ΔBDBR	ΔT	ΔBDBR	ΔT	ΔBDBR	ΔT	ΔBDBR	ΔT
Balloons	+0.65	-35.88	+0.25	-30.70	+0.49	-34.68	+0.72	-43.33
Kendo	+0.43	-39.50	+0.28	-35.99	+0.22	-41.59	+0.50	-49.41
Newspaper	+0.91	-34.79	+0.33	-27.08	+0.68	-31.03	+1.01	-40.45
GT_Fly	+0.28	-43.00	+0.10	-51.10	+0.19	-50.46	+0.29	-57.60
Poznan_Hall2	+1.12	-48.88	+0.58	-55.09	+1.01	-61.87	+1.41	-66.07
Poznan_Street	+0.30	-42.66	+0.15	-36.58	+0.18	-43.35	+0.32	-51.13
Shark	+0.42	-37.44	+0.03	-43.92	+0.33	-42.09	+0.41	-50.87
Undo_Dancer	+0.42	-41.74	+0.24	-45.30	+0.53	-47.52	+0.42	-41.74
Average	**+0.57**	**-40.49**	**+0.25**	**-40.72**	**+0.45**	**-44.07**	**+0.64**	**-50.08**

where the $\widehat{Flag}_{Split}$ of 0 and 1 represent Non-Split and Split of the current CU in our proposed algorithm, respectively.

Besides, our proposed algorithm does not affect the mode decision for CUs at each depth level, which means our algorithm could be integrated with other fast mode decision methods at each depth level for further acceleration.

V. SIMULATION RESULTS

The proposed early termination for fast intra mode decision in depth map coding has been implemented in HTM-16.1 [33]. The original depth intra mode decision in HTM-16.1 was an anchor for comparison with the algorithms in [26, 29] and the proposed algorithm. The quantization parameters (QPs) were set as 25, 30, 35, 40 for texture views and 34, 39, 42, 45 for the corresponding depth views. All results in Table V-VI are the average simulation results of these QPs. Test sequences include *Kendo*, *Balloons*, *Newspaper*, *GT_Fly*, *Poznan_Hall2*, *Poznan_Street*, *Undo_Dancer*, and *Shark*. 100 frames of each sequence were tested under the common test condition (CTC) specified in [34]. Since our method was designed for intra coding, the coding configuration is All-Intra. The experimental work was implemented on the platform with the CPU of Intel(R) Core i7-4790 CPU @ 3.60GHz and RAM 16.0GB.

A. Precision and Recall of our Proposed Classification

In this paper, the decision of early termination can be considered as a binary classification problem, in which the CUs would not be coded at the higher depth level using (5) in the final bitstream (i.e. terminated at the current or lower depth) are treated as true labels. Besides, based on the analysis of DIS-inheritance above, we believe that the partitioning process could be terminated immediately using (17) when a DIS-parent CU is detected after the VSO and AVSO processes. Therefore, the DIS-parent CUs are considered as predicted true labels. To further verify the performance of the proposed classification based on DIS-inheritance, true positive (TP), false positive (FP), false negative (FN) and true negative (TN) are defined in the confusion matrix in Table V. Table VI then shows its precision and recall at various depth levels in which the precision and the recall are calculated using *TP*, *FP* and *FN* as follows:

$$Precision = \frac{TP}{TP+FP}, \qquad Recall = \frac{TP}{TP+FN} \tag{18}$$

From (18) and Table V, it can be seen that precision is the accuracy among all predicted positive CUs and recall is the fraction of the correctly predicted positive CUs that have been successfully detected over the total number of actual positive CUs. It is noted that the classification with higher precision implies a lower increase in BDBR [18]. Besides, the recall of the proposed classification affects the time reduction of our fast method only but does not increase the BDBR.

From Table VI, it can be observed that this DIS-inheritance based binary classification has high precision at each depth level, especially for the depth level from 1 to 3 (99.17%-99.99%). The slightly lower precision at the depth level of 0 mainly results from two reasons. First, large CUs of 64×64 pixels contain discrete details, which could be predicted well in a smaller size. Second, it is found in Table III that $P(\hat{m}_1^i \in M_0)$ is less accurate (even it is already 90.44%), as compared with $P(\hat{m}_2^i \in M_1)$ and $P(\hat{m}_3^i \in M_2)$. When the estimation of the most probable candidate list is not accurate enough, the mismatch between depth levels may introduce decision inaccuracy. Besides, the recall ranging from 49.20% to 74.42% also shows that the proposed classification based on DIS-inheritance could terminate over half of unnecessary partitioning with high precision. It is noted that the recall here refers to the proportion of DIS-parent CUs detected successfully. The DIS-parent CUs, which are not be detected

here, perform the original intra coding process and will not affect the coding quality.

B. Performance of our Proposed Algorithm

To further study the performances of the proposed algorithms compared with the state-of-the-art algorithms, coding results including complexity reduction and coding efficiency are taken into account. The average encoding time saving ΔT for four different QPs is used to evaluate the complexity reduction. And the coding efficiency is evaluated by BDBR [35], which is calculated by the PSNR of synthesized views and the total bitrate of depth and texture videos.

Table VII shows the experiment results of the proposed algorithms and the algorithms in [26,29]. The SEDV and PBED are two different fast mode decision methods in [26], which could achieve 14.74% and 31.83% of time reduction with little increase in BDBR. The SEDV only focuses on simplifying the DMM search process, which limits its time reduction, while the PBED method relies on the minimum VSD-based VSO cost of 35 CHIMs. On the other hand, the fast block partition algorithm in [29] is to limit depth coding quadtree by the coded texture quadtree. Although the time reduction of [29] is remarkable (over 50%), the BDBR increase is also beyond a normal acceptable interval, which mainly results from the mismatch between the depth map and texture image in intra coding.

As we can see in Table VII, our new proposed algorithm (PRO) could achieve 36.35% of time reduction with only 0.35% increase in BDBR, which maintains the best balance of coding efficiency and computation complexity than the other algorithms. Furthermore, due to the slightly lower precision in large CUs of 64×64 pixels as mentioned in Table V, we could restrict the proposed technique within depth level of 1 to 3. The performance of the restricted version is also shown in Table VI, named as "Restrict-PRO". Compared to the proposed algorithm for all depth levels, "Restrict-PRO" has better BDBR performance, 0.07% increase in average, while the coding time of "Restrict-PRO" is only slightly increased.

In addition, our proposed algorithm can be integrated with other fast mode decision algorithms at each depth level as mentioned in Section IV-C. Since the accumulated degradation will occur if different algorithms are combined, it is worth keeping the influence on the coding performance of each algorithm as low as possible. Due to the better performance in BDBR, the proposed "Restrict-PRO" is selected here to be integrated with fast mode decision algorithms in [26]. Compared to the performance of SEDV and PBED, the combined algorithms including SEDV+Restrict-PRO, PBED+Restrict-PRO, and SEDV+PBED+Restrict-PRO are shown in Table VIII. Specifically, the total integration remarkably reduces 50.08% of coding complexity with acceptable BDBR loss of 0.64%, which is better that of [29] with similar complexity reduction.

To further demonstrate the superiority of the proposed algorithms, Table IX further shows the comparison between our algorithms and some of the fast algorithms [10], [12-13], [25-29] according to different categories. It is noted that, except for [26] and [29] conducted in HTM-16.1 above, all algorithms in Table IX are from the simulation results shown in the corresponding reference papers. From Table IX, it is observed that our proposed algorithms can provide the best balance between time saving and ΔBDBR in the category of CU partition decision, as compared with the algorithms in [27-29]. Together with the fast PU mode decision methods in [26], our SEDV+PBED+Restrict-PRO can attain time reduction of 50.08%, which is better than [10], [12-13], and [25-26], while maintaining an acceptable increase of 0.64% in BDBR. Besides, compared with SEDV or PBED, the BDBR has an only slight increase in SEDV+Restrict-PRO (0.12% to 0.25%) or PBED+Restrict-PRO (0.37% to 0.45%), which mainly results from the negligible 0.07% BDBR increase of our Restrict-PRO. This kind of slight accumulated BDBR degradation cannot be achieved with the algorithms in [27] or [29], where the BDBR increase 0.44% or 3.13% cannot be ignored for combined methods. In addition, the BDBR for our combined method can be further controlled if the selected fast PU mode method has a lower increase in BDBR. Therefore, it can be concluded that our method can achieve better results than the current fast algorithms for intra mode decision in depth map coding.

TABLE IX PERFORMANCE OF PROPOSED ALGORITHMS COMPARED WITH PREVIOUS WORKS IN DIFFERENT CATEGORIES

Category	Works	ΔBDBR(%)	ΔT(%)
PU Mode Decision	Gu's [10] vs HTM-7.0	+0.30	-34.40
	Zhang's [12] vs HTM-5.1	+0.90	-40.30
	Park's [13] vs HTM-9.1	+0.13	-22.19
	Sanchez's [25] vs HTM-16.0	+0.10	-23.90
	SEDV in [26] vs HTM-16.1	+0.12	-14.74
	PBED in [26] vs HTM-16.1	+0.37	-31.83
CU Partition Decision	Zhang's [27] vs HTM-13.0	+0.44	-41.00
	Kim's [28] vs HTM-12.0	+0.18	-25.63
	Mora's [29] vs HTM-16.1	+3.13	-50.92
	PRO vs HTM-16.1	**+0.35**	**-36.35**
	Restrict-PRO vs HTM-16.1	**+0.07**	**-31.04**
CU+PU Decision	**SEDV+Restrict-PRO vs HTM-16.1**	**+0.25**	**-40.72**
	PBED+Restrict-PRO vs HTM-16.1	**+0.45**	**-44.07**
	SEDV+PBED+Restrict-PRO vs HTM-16.1	**+0.64**	**-50.08**

VI. CONCLUSIONS

In this paper, we have proposed an early determination algorithm for intra mode decision in depth map coding based on DIS-inheritance. The relationship between the DIS-inheritance and mode decision is discovered in this work. It is found that, for CUs well predicted by DIS at the low depth level, its sub-CUs at the higher depth level are likely to be coded by DIS due to the DIS-inheritance. Consequently, the recursive partitioning process is early terminated for CUs which have a DIS-parent CU at the higher depth levels. The detection of DIS-parent CUs is measured by evaluating the performance of DIS mode in the VSO and the new AVSO simultaneously. The AVSO is a fast and simple process to estimate the best prediction mode for the sub-CUs at the previous depth level, which facilitates the detection of DIS-parent CU. Experimental results show that the proposed algorithm can provide about 50.08% of time reduction with 0.64% BDBR loss together with other fast intra mode decision algorithms.

REFERENCES

[1] G. Tech, Y. Chen, K. Muller, J. R. Ohm, A. Vetro, and Y. K. Wang, "Overview of Mutiview and 3D Extensions of High Efficiency Video Coding," *IEEE Trans. Circuits Syst. Video Technol.*, vol. 26, no. 1, pp. 35-49, Jan. 2016.

[2] G. J. Sullivan, J. R. Ohm, W. J. Han, and T. Wiegand, "Overview of the High Efficiency Video Coding (HEVC) Standard," *IEEE Trans. Circuits Syst. Video Technol.*, vol. 22, no. 12, pp. 1649-1668, Dec. 2012.

[3] I. Kim, J. Min, T. Lee, W. J. Han, and J. Park, "Block Partitioning Structure in the HEVC Standard," *IEEE Trans. Circuits Syst. Video Technol.*, vol. 22, no. 12, pp. 1697-1706, Dec. 2012.

[4] J. Lainema, F. Bossen, W. J. Han, J. Min, and K. Ugur, "Intra Coding of the HEVC Standard," *IEEE Trans. Circuits Syst. Video Technol.*, vol. 22, no. 12, pp. 1792-1801, Dec. 2012.

[5] J. Y. Lee, M. W. Park, and C. Kim, "3D-CE1: Depth Intra Skip (DIS) Mode," Joint Collaborative Team on 3D Video Coding Extension Development (JCT-3V), JCT3V-K0033, pp. 1-5, Geneva, Switzerland, Feb. 2015.

[6] P. Merkle, K. Müller, and T. Wiegand, "Coding of Depth Signals for 3D Video Using Wedgelet Block Segmentation with Residual Adaptation," in *Proc. of IEEE Int. Conf. on Multimedia and Expo (ICME)*, pp. 1-6, San Jose, CA, USA, Jul. 2013.

[7] H. Liu and Y. Chen, "Generic Segment-Wise DC for 3D-HEVC Depth Intra Coding," in *Proc. of Int. Conf. on Image Process. (ICIP)*, pp 3219–3222, Paris, France, Oct. 2014.

[8] O. Stankiewicz, K. Wegner, and M. Domanski, "Impact of View Synthesis Optimization (VSO) on Depth Quality," Joint Collaborative Team on 3D Video Coding Extension Development (JCT-3V), JCT2-A0090, pp. 1-3, Stockholm, Sweden, Jul. 2012.

[9] Z. Gu, J. Zheng, N. Ling, and P. Zhang, "Fast Depth Modeling Mode Selection for 3D HEVC Depth Intra Coding", in *Proc. of IEEE Int. Conf. on Multimedia and Expo (ICME)*, pp. 1-4, San Jose, CA, USA, Jul. 2013.

[10] Z. Gu, J. Zheng, L. Nam, and P. Zhang, "Fast Bi-partition Mode Selection for 3D HEVC Depth Intra Coding," in *Proc. of IEEE Int. Conf. on Multimedia and Expo (ICME)*, pp. 1-6, Chengdu, China, Jul. 2014.

[11] T. L. da Silva, L. V. Agostini, and L. A. da Silva Cruz, "Complexity Reduction of Depth Intra Coding for 3D Video Extension of HEVC," in *Proc. of IEEE Int. Conf. on Visual Comm. and Image Process. (VCIP)*, pp. 229-232, Valletta, Malta, Dec. 2014.

[12] Q. Zhang, N. Li, L. Xun, and Y. Gan, "Effective Early Terminate Algorithm for Depth Map Intra Coding in 3D-HEVC," *Electron. Lett.*, vol. 50, no. 14, pp. 994-996, Jul. 2014.

[13] C. S. Park, "Edge-Based Intramode Selection for Depth-Map Coding in 3D-HEVC," *IEEE Trans. Image Process.*, vol. 24, no. 1, pp. 155-162, Jan. 2015.

[14] G. Sanchez, M. Saldanha, G. Balota, B. Zatt, M. Porto, and L. Agostini, "Complexity Reduction for 3D-HEVC Depth Maps Intra-Frame Prediction Using Simplified Edge Detector Algorithm," in *Proc. of Int. Conf. on Image Process. (ICIP)*, pp. 3209-3213, Paris, France, Oct. 2014.

[15] C.-H. Fu, H.-B. Zhang, W.-M. Su, S.-H Tsang, and Y.-L. Chan, "Fast Wedgelet Pattern Decision for DMM in 3D-HEVC," in *Proc. of IEEE Int.Conf. Digital Signal Process. (DSP)*, pp.477-481, Singapore, Jul. 2015.

[16] H.-B. Zhang, C.-H. Fu, Y.-L. Chan, S.-H. Tsang, W.-C. Siu, and W.-M. Su, "Efficient Wedgelet Pattern Decision for Depth Modeling Modes in Three-Dimensional High-Efficiency Video Coding," *J. Electron. Imag.*, vol. 25, no.3, pp. 033023.1-13, May-Jun. 2016.

[17] P. Merkle, K. Müller, X. Zhao, Y. Chen, L. Zhang, and M. Karczewicz, "CE6.H Results on Simplified Wedgelet Search for DMM Modes 1 and 3", Joint Collaborative Team on 3D Video Coding Extension Development (JCT-3V), JCT3V-B0039, pp. 1-7, Shanghai, China, Oct. 2012.

[18] M. Zhang, C. Zhao, J. Xu, and H. Bai, "A Fast Depth-Map Wedgelet Partitioning Scheme for Intra Prediction in 3D Video Coding," in *Proc. of IEEE Int. Symp. on Circuits Syst. (ISCAS)*, pp. 2852-2855, Beijing, China, May 2013.

[19] G. Sanchez, M. Saldanha, G. Balota, B. Zatt, M. Porto, and L. Agostini, "A Complexity Reduction Algorithm for Depth Maps Intra Prediction on the 3D-HEVC," in *Proc. of IEEE Int. Conf. on Visual Comm. and Image Process. (VCIP)*, pp. 137-140, Valletta, Malta, Dec. 2014.

[20] L. F. R. Lucas, K. Wegner, N. M. M. Rodrigues, C. L. Pagliari, E. A. B. da Silva, and S. M. M. de Faria, "Intra Predictive Depth Map Coding Using Flexible Block Partitioning," *IEEE Trans. Image Process.*, vol. 24, no. 11, pp. 4055-4068, Nov. 2015.

[21] C. Y. Li, X. J, and Q. H. Dai, "A Novel Distortion Model for Depth Coding in 3D-HEVC," in *Proc. of Int. Conf. on Image Process. (ICIP)*, pp. 3228 – 3232, Paris, France, Oct. 2014.

[22] B. T. Oh, and K. J. Oh, "View Synthesis Distortion Estimation for AVC- and HEVC-Compatible 3-D Video Coding," *IEEE Trans. Circuits Syst. Video Technol.*, vol. 24, no. 6, pp.1006-1015, Jun. 2014.

[23] Z. Gu, J. Zheng, N. Ling, and P. Zhang, "Fast Intra SDC Coding for 3D-HEVC Intra Coding," Joint Collaborative Team on 3D Video Coding Extension Development (JCT-3V), JCT3V-I0123, pp. 1-5, Sapporo, japan, Jul. 2014.

[24] J. Y. Lee, M. W. Park, Y. Cho, and C. Kim, "3D-CE2 related: Fast SDC DC Offset Decision," Joint Collaborative Team on 3D Video Coding Extension Development (JCT-3V), JCT3V-I0084, pp. 1-2, Sapporo, Japan, Jul. 2014.

[25] G. Sanchez, L. Agostini, and C. Marcon, "Complexity Reduction by Modes Reduction in RD-List for Intra-Frame Prediction in 3D-HEVC Depth Maps," in *Proc. of IEEE Int. Symp. on Circuits Syst. (ISCAS)*, pp. 1-4, Baltimore, MD, USA, May, 2017.

[26] H.-B. Zhang, C.-H. Fu, Y.-L. Chan, S.-H. Tsang, and W.-C. Siu, "Probability-based Depth Intra Mode Skipping Strategy and Novel VSO Metric for DMM Decision in 3D-HEVC," *IEEE Trans. Circuits Syst. Video Technol.*, vol. 28, no. 2, pp. 513-527, Feb. 2018.

[27] H.-B. Zhang, Y.-L. Chan, C.-H. Fu, S.-H. Tsang, and W.-C. Siu, "Quadtree Decision for Depth Intra Coding in 3D-HEVC by Good Feature," in *Proc. of IEEE Int. Conf. on Acoustics, Speech and Signal Process. (ICASSP)*, pp.1481-1485, Shanghai, China, Mar. 2016.

[28] M. Kim, N. Lim, and L. Song, "Fast Single Depth Intra Mode Decision for Depth Map Coding in 3D-HEVC," in *Proc. of IEEE Int. Conf. on Multimedia and Expo (ICME)*, pp. 1-6, Turin, Italian, Jun. 2015.

[29] E. G. Mora, J. Jung, M. Cagnazzo and B. Pesquet, "Initialization, Limitation, and Predictive Coding of the Depth and Texture Quadtree in 3D-HEVC," *IEEE Trans. Circuits Syst. Video Technol.*, vol. 24, no. 9, pp. 1554-1565, Sep. 2014.

[30] G. Tech, H. Schwarz, K. Müller, T. Wiegand, "3D Video Coding Using the Synthesized View Distortion Change," in *Proc. of Picture Coding Symp. (PCS)*, pp. 25-28, Krakow, Poland, May 2012.

[31] B. T. Oh, J. Lee, and D. s. Park, "Depth Map Coding Based on Synthesized View Distortion Function," *IEEE J. Sel. Topics. Signal Process*, vol. 5, no.7, pp. 1344-1352, Oct. 2011.

[32] Y. Chen, G. Tech, K. Wegner, and S. Yea, "Test Model 11 of 3D-HEVC and MV-HEVC," Joint Collaborative Team on 3D Video Coding Extension Development (JCT-3V), JCT3V-K1003, pp. 1-76, Geneva, Switzerland, Feb. 2015.

[33] 3D-HEVC Reference Software: "HTM-16.1," [Online]. Available at https://hevc.hhi.fraunhofer.de/svn/svn_3DVCSoftware/tags/HTM-16.1/

[34] K. Müller, and A. Vetro, "Common Test Conditions of 3DV Core Experiments," Joint Collaborative Team on 3D Video Coding Extension Development (JCT-3V), JCT3V-G1100, pp. 1-7, San Jose, CA, USA, Jan. 2014.

[35] G. Bjøntegaard, "Calculation of Average PSNR Differences Between RD Curves," ITU-T Video Coding Experts Group (VCEG), VCEG-M33, pp. 1-4, Austin, Texas, USA, Apr. 2001.